Diagnostic Comparison of Wintertime East Asian Subtropical Jet and Polar-Front Jet: Large-Scale Characteristics and Transient Eddy Activities*

REN Xuejuan[1†](任雪娟), YANG Xiuqun[1](杨修群), ZHOU Tianjun[2](周天军), and FANG Jiabei[1](房佳蓓)

1 *Institute of Severe Weather and Climate, School of Atmospheric Sciences, Nanjing University, Nanjing* 210093

2 *National Key Laboratory of Numerical Modeling for Atmospheric Sciences and Geophysical Fluid Dynamics (LASG), Institute of Atmospheric Physics, Chinese Academy of Sciences, Beijing* 100029

(Received April 13, 2010)

ABSTRACT

Diagnostic comparison of the East Asian subtropical jet (EASJ) and polar-front jet (EAPJ) in winter season is carried out by using the ERA-40 dataset. The large-scale circulation characteristics and synoptic-scale transient eddy activities (STEAs) associated with the EASJ and EAPJ are examined. The results show that the EASJ and EAPJ in the upper-level monthly mean data have no clear geographical border, while the distribution of the numbers of jet cores from the daily data exhibits a distinct boundary at the latitudes of the northern Tibetan Plateau. The two areas with large numbers of jet cores correspond to the EASJ and EAPJ regions. The analysis of STEAs over the East Asian region shows a spatial match of STEAs with the EASJ and EAPJ in winter: the strong EASJ is located within the weak southern branch of the STEA while the relatively weak EAPJ appears within the active northern branch of the STEA, indicating that the EAPJ is the jet coexisting with the STEA. Further analysis shows two anomalous modes of the winter EAPJ: the anomalous anticyclonic/cyclonic circulation and the weakened/strengthened local westerly wind. The large-scale circulation anomalies in the Northern Hemisphere related to the first mode are concentrated in the Eurasian mid to high latitudes, and are also influenced by the anomalous circulation in the upstream area. When the local westerly wind over the EAPJ region is weakened/strengthened, the westerly jet in the eastern part of the EASJ and that in the western Pacific region show opposite variations. The corresponding anomalous atmospheric circulation demonstrates the Eurasian (EU) pattern. The EAPJ anomalies are also closely linked with the STEA anomalies over East Asia. The anomalies in the northern branch of the STEA propagate as a wave train along its axis into the East Asian coastal waters, and then migrate eastward to the oceanic region. However, the ones near the southern branch are trapped over the eastern part of East Asia and its coastal waters at 200 hPa.

Key words: East Asian subtropical jet, East Asian polar-front jet, diagnostic comparison, synoptic-scale transient eddy activities

Citation: Ren Xuejuan, Yang Xiuqun, Zhou Tianjun, et al., 2011: Diagnostic comparison of wintertime East Asian subtropical jet and polar-front jet: Large-scale characteristics and transient eddy activities. *Acta Meteor. Sinica*, **25**(1), 21–33, doi: 10.1007/s13351-011-0002-2.

1. Introduction

The upper-troposphere jet stream circumnavigating the globe is one of the important members in the midlatitude circulation system. According to the observational results, there exists a state of two jets – the subtropical jet and the polar-front jet (also referred to as subpolar jet or eddy-driven jet). Over the East Asian region in the winter season, the two jets are located zonally along the southern side of the Tibetan Plateau (TP) and 40°–60°N poleward side of the TP, respectively. They are termed as the East Asian subtropical jet (EASJ) and the East Asian polar-front jet (EAPJ), respectively (Sheng, 1986; Zou et al., 1990). After the confluence of the two jets over the East Asian coastal waters, the joint jet reaches its maximum intensity over the southeast of Japan Island and extends eastward into the oceanic region with gradually

*Supported by the National Natural Science Foundation of China under Grant Nos. 40775044 and 40730953, and the Natural Science Foundation of Jiangsu Province under Grant No. BK2008027.

†Corresponding author: renxuej@nju.edu.cn.

(Chinese version published in Vol. 68, No. 1, 1–11, 2010)

reduced intensity. The term "western Pacific jet stream" (WPJ) was used to denote the jet stream over the midlatitude Pacific Ocean (Cressman, 1981). Because the dominant direction of the jet stream over East Asia–Pacific is zonally westerly, the literature also generally refers to it as East Asian westerly jet stream (Yang et al., 2002; Mao et al., 2007).

As an important circulation system over the East Asian-Pacific region and one of the strong signals for the anomalous precipitation over eastern China, the westerly jet stream (Sheng, 1986; Zou et al., 1990; Zhang et al., 2006), its seasonal variation and its relationships to ENSO (Yang et al., 2002) and East Asian monsoon have been studied extensively (Yang et al., 2002; Jhun and Lee, 2004; Li et al., 2004; Liao et al., 2004; Wang et al., 2002; Sun et al., 2002; Zhou et al., 2003; Kuang and Zhang, 2006; Mao et al., 2007), It is shown that when the EASJ jumps from the south to the north side of the TP in mid-June, the EAPJ disappears over the north side of the TP; the withdrawal of the EASJ in mid-October is accompanied by the appearance of the EAPJ over the north side of the TP. These phenomena reflect the seasonal variation of the East Asian atmospheric circulation (Ye et al., 1958; Sheng, 1986; Zou et al., 1990). On the interannual variation timescale, the wintertime westerly jet over East Asia demonstrates changes in both its intensity and its location (south-north shifts). These variations impact on the temperature and precipitation over China via the winter monsoon (Mao et al., 2007). The variation of the westerly jet stream over East Asia–western Pacific is opposite in phase to that in the EAPJ region. Both of them are closely related to the East Asian winter monsoon (Jhun and Lee, 2004; Mao et al., 2007). The variations of the wintertime WPJ intensity are linked with the winter climate anomalies over the entire East Asian-Pacific-North American region. A strong WPJ is associated with an intensification of the East Asian winter monsoon. The colder and drier conditions directly reduce the surface air temperature over East Asia (Yang et al., 2002). The East Asian jet stream also serves as a link between Atlantic-European and East Asian climate anomalies. The signal of the North Atlantic Oscillation (NAO) can propagate eastward along the jet stream as waveguide and extend into East Asian and North Pacific region, therefore, leading to climate anomalies over East Asia in winter and spring (Watanabe, 2004; Yu and Zhou, 2004, 2007; Li et al., 2005; Xin et al., 2006). Many factors can cause the anomalies of the East Asian jet stream. For example, the anomalies of the Hadley Cell can induce anomalous zonal wind in midlatitudes (Hou, 1998); the interaction between wave and jet stream can yield the acceleration of the jet stream (Gao et al., 1989). In addition, the anomalous snow cover over the Eurasian region (Chen and Sun, 2003; Chen et al., 2003) and the anomalous convection over the tropical region (Dong et al., 1999) are also closely connected with the East Asian jet stream anomalies.

The jet stream over East Asia–Pacific is also associated with the synoptic-scale transient eddy activities (STEAs) (Wu et al., 2006; Ren and Zhang, 2007). One of the strongest atmospheric baroclinic zones on the globe lies over the East Asian coastal waters to midlatitude North Pacific regions due to the jet stream. Thus, the STEAs in this region are more active than those in other latitudes. Two branches of the STEA are located over the East Asian landmass (Tao and Hu, 1994). They join together over the East Asian coastal region and the northern part of Japan Island. After the confluence, they enhance robustly and extend eastward to the northwest coastal region of North America. The maximum STEA belt is located on the northeast side of the jet stream over the oceanic region (Zhu and Sun, 2000; Ren and Zhang, 2007). Observational and theoretical studies over the last 10 years have suggested that the STEA anomalies demonstrate a symbiotic relationship with the westerly jet stream anomalies over the Pacific region, via a local positive dynamical feedback (Carillo, 2000; Ren and Zhang, 2007). In addition, the anomalous "seeds"–the STEA anomalies over East Asia can influence the transient eddy activities over the oceanic region through downstream and baroclinic development mechanisms, resulting in the jet stream anomalies over the oceanic region (Orlanski, 2005).

The observational results have shown that the wintertime EAPJ is much weaker than the EASJ and WPJ. The EASJ and EAPJ exhibit no distinct geographical border in the upper-level monthly wind field. Consequently, the comparison of the EASJ and EAPJ is lacking. The variation features of EAPJ and associated mechanism are not clear. Moreover, because the STEA over the East Asian landmass are less active than those over the oceanic region, few studies have focused on its relationships to EASJ and EAPJ over the landmass. In this study, we investigate and compare the climatological features and interannual variations of EASJ and EAPJ by examining both the large-scale circulation patterns and the STEA. We also explore the associated variations of the STEA. These will help to understand the climate variations and their mechanism over East Asian-North Pacific regions.

2. Data and analysis methodology

The atmospheric reanalysis data (ERA 40) of the European Center for Medium-range Weather Forecasts (ECMWF; Uppala et al., 2005) are used. Daily and monthly mean fields, with a spatial resolution of $2.5°\times2.5°$ in latitude and longitude, covering the period from September 1, 1957 to August 31, 2002 are selected. Winter is defined as December-January-February (DJF).

To investigate the features of transient eddy activities linked with the jet stream, the STEA kinetic energy and the number of jet cores per month at each grid point are calculated using 0000 and 1200 UTC daily upper-level wind fields. A jet core at 300 hPa is defined if (1) the wind speed v in the East Asian-North Pacific region (20°–70°N, 60°E–140°W,) is equal to or greater than 30 m s^{-1}, and (2) the wind speed is the local maximum of the surrounding 24 grid points. The corresponding latitude and longitude of the jet core are recorded. The above counting procedure is repeated for every day in winter season. For a specific winter, the number of jet cores is noted as n at a certain grid point where n jet cores are identified totally by inspection of the wind speed in this winter period. The STEA kinetic energy is calculated by $k_{\rm e}=\frac{1}{2}\overline{(u'^2+v'^2)}$, where u and v denote the zonal and meridional wind velocities; the overbar represents the mean value in winter, and the primes denote perturbations with periods of 2.5–8 days. Our results have shown that the location and intensity of $k_{\rm e}$ can also represent the STEA features in mid latitudes, similar to the STEA defined by geopotential height and meridional wind.

The empirical orthogonal function (EOF), linear regression and correlation methods are used in this study.

3. Climatological distributions of wintertime EASJ, EAPJ, and STEA

Figure 1 shows the latitude-height cross-sections of the climatological winter wind speed and relative vorticity. The longitudes of the sections span over the TP and to the east of the TP, respectively. Both sections exhibit the EASJ jet core at 200 hPa, with the wind intensity larger than 40 m s^{-1}. Below the jet core, the wind intensity decreases dramatically. The wind structure in the EAPJ region in the northern TP shows considerable differences from that in the EASJ region. No closed wind center appears distinctly in the EAPJ area in the whole troposphere. Only one cone-like wind belt stretches downward from the upper level to the lower level. Above 700 hPa, the vertical wind shear in the EASJ region is much stronger than that in the EAPJ region, while it is the opposite below 700 hPa. The zero line of relative vorticity is located around 30°N. South of the zero line is prevailed by an anticyclonic circulation pattern in the whole troposphere, while north of it is anchored by a cyclonic pattern at the mid-upper level.

Figure 1 also shows that the EASJ and EAPJ in the upper-level wind field exhibit no distinct geographical border on the climatological mean. Meanwhile, there is no jet core for the EAPJ at the upper level. These features are in sharp contrast with the subtropical jet and polar-front jet in the Southern Hemisphere (Teresa et al., 2001; Gallego et al., 2005). In fact, on the daily weather map, several jet cores scatter along the meandering jet stream belt. Figure 2 displays the distribution of the numbers of the jet cores at 300 hPa

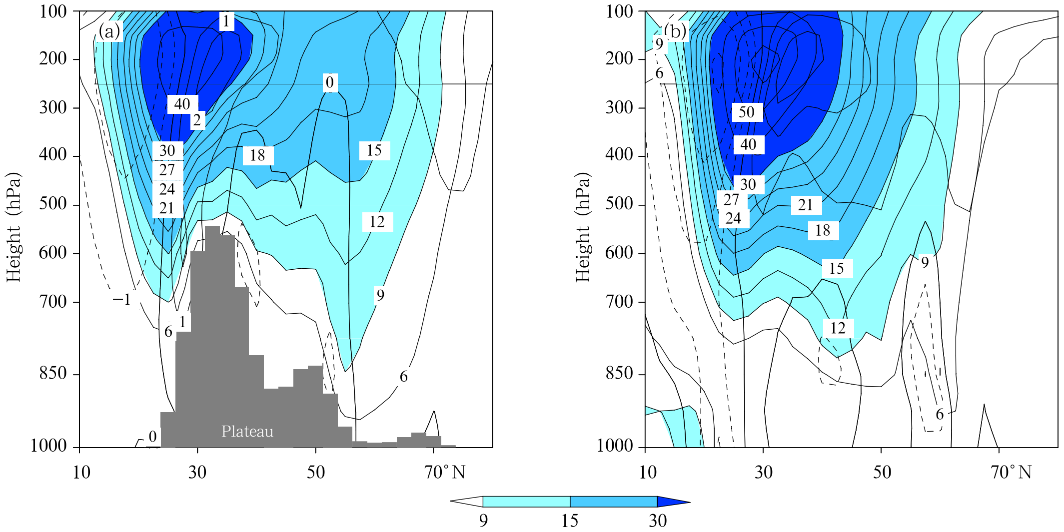

Fig. 1. Climatological winter mean latitude-height cross-sections of wind speed (thin line and shaded area) and relative vorticity (thick line) (a) averaged over 70°–100°E and (b) along 115°E. The intervals of wind speed are 3 and 10 m s^{-1} respectively for the wind speeds smaller than 30 m s^{-1} and larger than 30 m s^{-1}. The interval of relative vorticity is 1×10^{-5} s^{-1}.

for climatological winter mean, which is obtained according to the identifying process in Section 2. The distribution of jet center numbers at 200 hPa is similar to that at 300 hPa (figure omitted). Figure 2 shows that the jet cores are concentrated mainly in two lobes. The narrow southern one is trapped zonally on the south flank of the TP and extends eastward to the east of the dateline, while the northern one is located in the square region of 40°–65°N poleward of the TP. It also stretches from northwest to southeast and gathers together with the southern one over the East Asian coastal region. Those two lobes are corresponding respectively to the EASJ and the EAPJ regions. Obviously, more jet cores are found in the southern lobe than in the northern lobe. A distinct area with minimum jet cores appears between the two lobes. This area extends zonally from the west side to the east side of the northern TP, indicating a clear geographical border between the two jet core lobes. This area can be considered as the border between the EASJ and EAPJ in winter.

Figure 3 shows the latitude-height sections of the

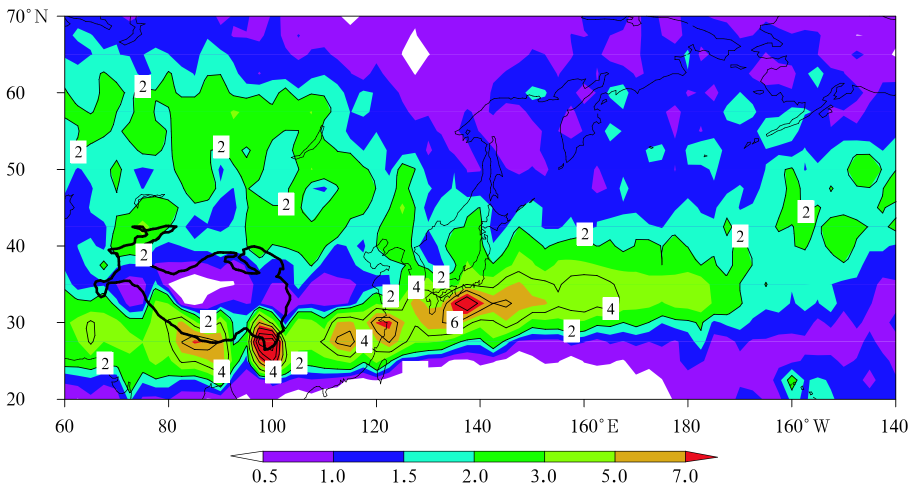

Fig. 2. Climatological winter mean jet core numbers at 300 hPa.

climatological winter STEA over the East Asian region. It is seen that there are two STEA maximum centers, corresponding respectively to the southern and northern STEA branches. The northern branch is stronger than the southern one. It is located poleward of the TP, with a closed center at 300 hPa. The southern branch is zonally elongated in a narrow region south of 35°N. It is more robust at 200 hPa. However, its intensity is only half of that of the northern branch. The STEA between the two branches is suppressed due to the topographic effect. When comparing the double jets and the two branches of the STEA in Figs. 1, 2, and 3, we can find that the EASJ, which is comparatively stronger than the EAPJ, is accompanied by the weak southern branch of the STEA, while the relatively weaker EAPJ is accompanied by the active northern branch of the STEA.

4. Variations of wintertime EASJ and EAPJ in connection with large-scale circulations and STEA anomalies

4.1 Variations of wintertime EASJ and EAPJ in connection with large-scale circulations

An EOF analysis is applied to the winter normalized 200-hPa u and v for the region 35°–75°N, 60°–130°E. The linear trend in the original wind data is subtracted at each grid point before the EOF analysis. The spatial patterns of the first two EOFs, and the time series of the corresponding principal components denoted as T1 and T2 respectively and measured in units of their respective standard deviation, are plotted in Fig. 4. The two modes explain 31.2% and 19.4% of the total interannual variance, respectively. The spatial pattern of the first EOF in Fig. 4 shows an anomalous anticyclonic/cyclonic circulation in the EAPJ region, while the second EOF depicts the weakening/strengthening of the westerly wind in the EOF domain.

To examine the large-scale circulation anomalies in the Northern Hemisphere in connection with the wintertime EAPJ anomalies, the principal components in Fig. 4 are used to select the positive and negative years for the two EOF modes, respectively, according to the 1.0 standard deviation of their time series T1/T2. The composite differences of the 200-hPa zonal wind and 500-hPa geopotential height in winter between the positive and negative years are constructed and plotted in Fig. 5. It is shown that large-scale circulation anomalies in the Northern Hemisphere appear in the mid to high latitudes over the Eurasian region, when the anomalous anticyclonic/cyclonic circulation occurs in the EAPJ region (the first EOF). Specifically, enhanced 500-hPa geopotential height in the EAPJ region, reduced westerly winds in the region from north side of the EASJ to 55°N, and intensified westerly winds in the high latitudes, are observed. In addition, anomalous westerly winds also occupy part of the Southeast and South

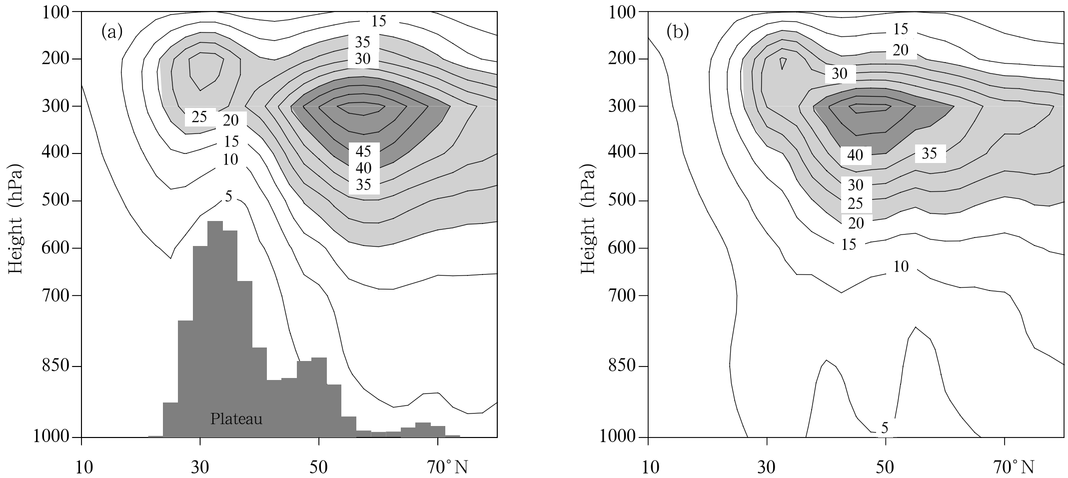

Fig. 3. As in Fig. 1, but for k_e of STEA ($m^2\ s^{-2}$).

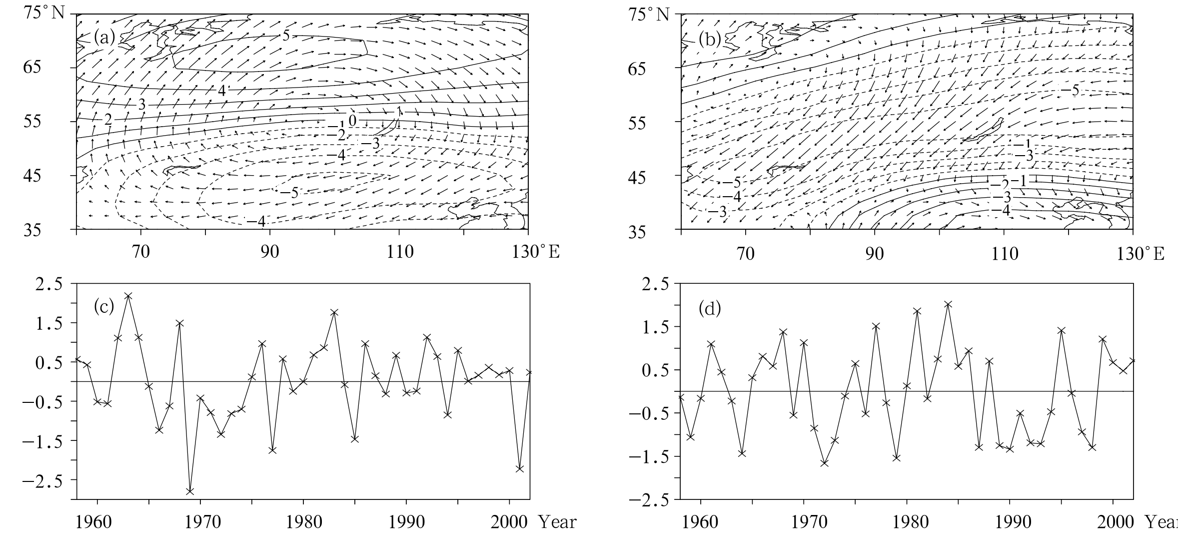

Fig. 4. Spatial patterns (upper panels) and normalized time coefficients (lower panels) of the first two leading EOF modes of the wind field at 200 hPa in winter. The isoline in (a) and (b) is the zonal component of the spatial pattern. The number "1960" on the abscissa in (c) and (d) indicates the winter of 1960.

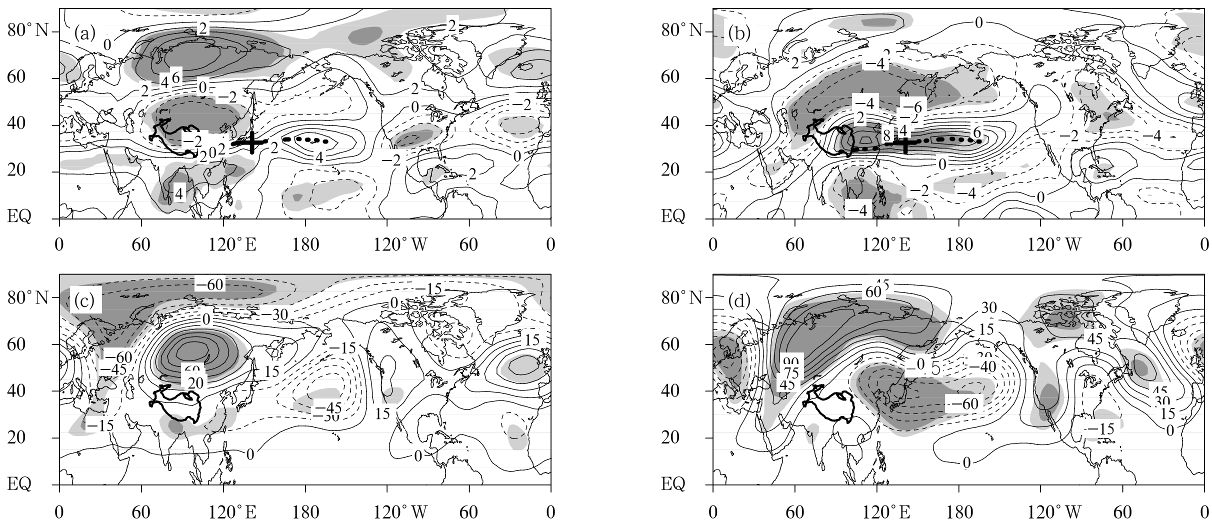

Fig. 5. Composite differences of the zonal wind at 200 hPa (upper panels; m s^{-1}) and geopotential height at 500 hPa (lower panels; gpm) in winter (positive minus negative). Statistically significant regions according to a t-test at α = 0.01 (0.05) level are denoted by dark (light) shading. Dark dotted lines and plus marks in (a) and (b) indicate the climatological westerly jet axis and jet center, respectively. (a, c) are for the first mode and (b, d) are for the second mode.

Asian region. With the weakening/strengthening of the westerly wind in the EAPJ region (the second EOF), the 500-hPa geopotential height field is characterized by a wave train from the European-Northwest Asian area to the East Asian (East Asian coastal) region. This is the Eurasian pattern (EU) defined by Wallace and Gutzler (1981). The high correlation coefficient of 0.86 between T2 and EU index also verifies this result. Meanwhile, in the composite differences of the zonal wind at 200 hPa, the variation of the westerly wind over the EAPJ region is opposite in phase to that over the East Asian-western Pacific region.

The upper-level zonal wind is often used to define jet stream indices in studies of the East Asian winter monsoon (Yang et al., 2002; Mao et al., 2007; Jhun and Lee, 2004). For example, Yang et al. (2002) defined the East Asian jet stream index (EAJSI) as the normalized winter 200-hPa u averaged within the area 30°–35°N, 130°–160°E. This index is significantly anti-correlated with the zonal wind intensity in the EAPJ region. Considering this correlation feature, Jhun and Lee (2004) defined a new East Asian winter monsoon index (EAWMI) as the difference in the area-averaged zonal wind speed at the 300-hPa level between the above two anti-correlated regions. Their results suggested that the EAWMI can well describe the variability of the winter monsoon in midlatitude East Asia. Mao et al. (2007) used the normalized winter 200-hPa u averaged over 30°–35°N, 127.5°–155°E as an intensity index of the East Asian jet stream, and the normalized 200-hPa u difference between two areas over 15°–25°N, 100°–115°E and 30°–40°N, 100°–115°E as the shear index, which can reasonably reflect the interannual variation of the intensity and meridional displacement of the East Asian jet stream, respectively. The correlation coefficients of T2 EAJSI, EAWMI, and Mao's intensity index are 0.73, 0.85, and 0.75, respectively. The high correlations suggest that the second EOF in Fig. 4 represents the weakening/strengthening of the westerly wind in the EAPJ region. Moreover, it also represents the strengthening/weakening of the westerly wind in the EASJ region. The correlation coefficient between T1 and Mao's shear index is 0.46, and it exceeds the 99% significance level ($\alpha_{0.01} = 0.37$). Thus, the first mode in Fig. 4 reflects the anomalous south-north movement of the EASJ.

Both the observation and simulation show that, via the radiative cooling effect, the anomalous snow cover in the mid-high Eurasian continent can modify the atmospheric temperature and geopotential height fields, and thus trigger the atmospheric EU teleconnection pattern in winter (Chen and Sun, 2003; Chen et al., 2003). Through the above process, the westerly wind in the EAPJ region is intensified/reduced and the one in the EASJ region is reduced/intensified, as shown in Fig. 4 for the second EOF mode. To understand the causative mechanisms of the second mode, the correlation coefficients between T1 and the eastern Atlantic pattern (EA) index (Wallace and Gutzler, 1981), and Detween T1 and the Arctic Oscillation (AO) index (Thompson and Wallace, 1998) are calculated and the results are 0.57 and –0.45, respectively. These results indicate that the anomalous anticyclonic/cyclonic circulation in the EAPJ region is linked with the atmospheric circulation anomalies both in mid to high latitudes and over the upstream region. To further explore these connections, the northern lobe and the southern lobe are chosen as 50°–65°N, 75°–115°E (mid to high latitudes) and 22.5°–30°N, 85°–120°E (subtropical region), respectively, and the 850–300-hPa temperature difference between the southern and northern lobes are calculated. A bigger difference indicates that the southern lobe is relatively warmer and the northern lobe is colder, which leads to intensification of westerly wind around 40°N over north side of the TP through the thermal wind relationship, and vice versa. Figure 6 shows the normalized time series of wintertime 850–300 hPa temperature difference between the southern and northern lobes defined above. The correlation coefficient of –0.94 between T1 and the temperature difference in

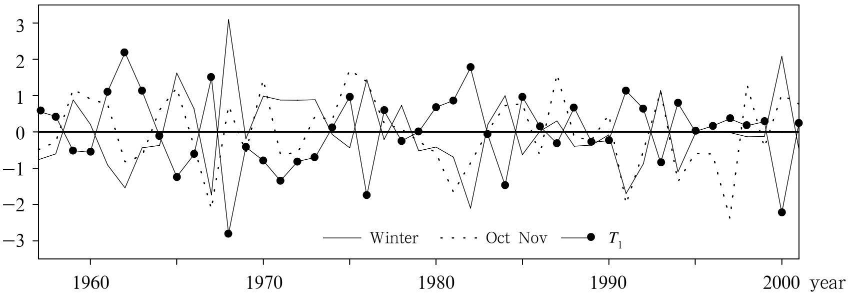

Fig. 6. Normalized time series of 850–300 hPa temperature difference between the southern area and northern area. The solid line is for winter, the dashed line is for October-November, and the solid-dotted line is for T1.

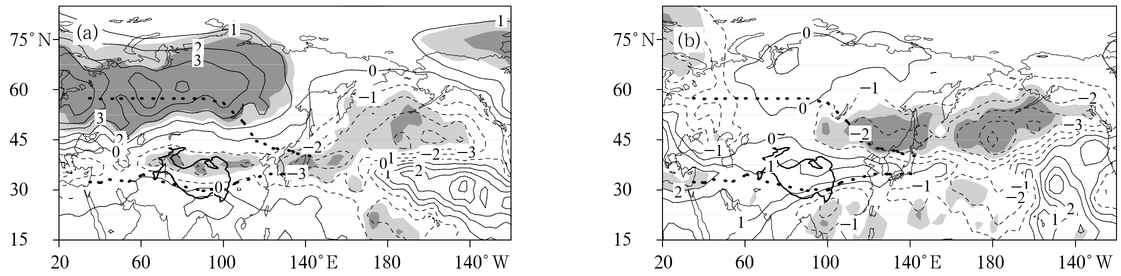

Fig. 7. Regressed fields of the winter STEA at 200 hPa against (a) T1 and (b) T2. Statistically significant regions according to a t-test at $\alpha = 0.01$ (0.05) level are denoted by dark (light) shading.

winter suggests that they bear opposite evolution features during the winters of 1957–2001. Further analysis shows that in October and November in the upstream region, there also exist a northern lobe and a southern one covering 50°–65°N, 60°–90°E and 27.5°–35°N, 60°–70°E, respectively. The normalized time series of the temperature difference between the upstream southern and northern lobes in October-November is also plotted in Fig. 6. The correlation coefficients of this temperature difference with T1 and the temperature difference in winter are –0.49 and 0.55, respectively. The results indicate that the atmospheric circulation anomalies in the mid to high latitudes and over the upstream of East Asia may cause the circulation anomalies in the EAPJ region through influencing the temperature contrast between the mid-high latitude Eurasia and the subtropical regions.

4.2 The STEA anomalies and their propagation features

Figure 7 shows the regressed patterns of wintertime STEA kinetic energy at 200 hPa against T1 and T2. It can be seen that the jet stream anomalies in winter are accompanied by the STEA anomalies over East Asia. For the first mode, the STEAs over the landmass north of 45°N are significantly increased/reduced, while the STEAs extending zonally from the northwestern TP to the East Asian coastal waters are noticeably reduced/increased. For the second mode, the STEA anomalies over the landmass are mainly concentrated over the northern branch region of the STEA.

The STEA anomalies over the landmass in Fig. 7 also extend to the midlatitude North Pacific. A previous investigation has demonstrated that the local atmospheric and oceanic circulation anomalies in the North Pacific region can generate local STEA anomalies (Zhu and Sun, 2000). Furthermore, a simulation study has shown that the eastward propagation of STEA anomalies over East Asia can also act to cause the STEA anomalies over the oceanic region downstream of East Asia (Orlanski, 2005). It is natural to ask whether the STEA anomalies over land, which are connected with the East Asian jet stream anomalies, can migrate eastward into the oceanic region by a certain way, and then lead to the STEA anomalies over the oceanic region. To answer this question, the maximum STEA anomaly centers over East Asian coastal waters in Figs. 7a and 7b are selected. They are the regions 35°–40°N, 135°–140°E (Fig. 7a, base point 1) and 42.5°–47.5°N, 145°–150°E (Fig. 7b, base point 2). Synoptic filtered daily v' in these two regions is averaged for every winter. Thus, two 90-day time series in one winter are constructed respectively for base points 1 and 2. The propagation features of wintertime STEA linked with these two base points can be detected by the lag-regression of 90-day spatial v' respectively with the two time series. The climatological propagation features are obtained via averaging the 45-winter regression fields. The positive/negative years selected in Section 4.1 according to T1/T2 are still used here to examine the composite structures. The composite structures give the different STEA propagation features respectively in the positive and negative years. This lag-regression method has been applied to investigating characteristics of baroclinic wave propagation and downstream development in winter (Lim and Wallace, 1991; Chang, 1993).

According to previous studies, the climatological STEA migration pattern is dominated by eastward propagation features (Lim and Wallace, 1991; Tao and Hu, 1994).

Figure 8 shows the climatological STEA migration pattern (left panels) and composite differences between positive and negative years (right panels). The number in the figure caption (–2 day, –1 day, 0, +1 day, +2 day) denotes lag days. The zero-lag means simultaneous regression. The negative number means that the spatial fields lag the time series of base points, while the positive number means that the spatial fields lead the time series. It can be seen in Fig. 8c that, at lag = 0, a wave train propagates eastward from the

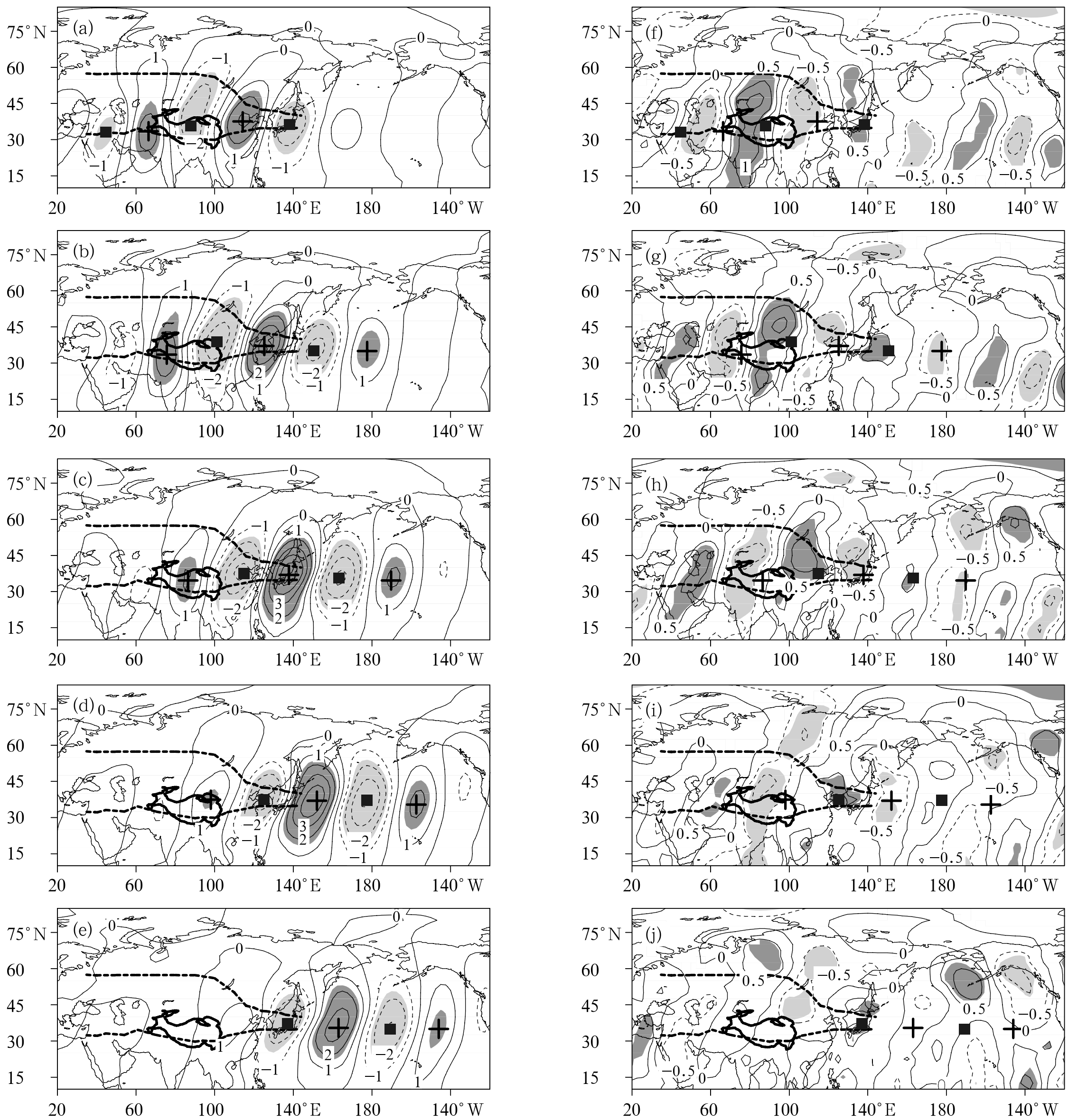

Fig. 8. Regression maps of 200-hPa synoptic-scale meridional wind for the base point 1. The left panels represent climatological mean, and the right panels represent composite difference of the first mode. The contour shows the regression value. Regions with values exceeding the 95% significance level are shaded. Signs "+" and "–" denote the centers of the wave trains for the climatological mean. Two dashed lines indicate the axes of the southern and northern branches of the STEA over East Asia, respectively. (a, f) for –2 day, (b, g) for –1 day, (c, h) for 0 day, (d, i) for +1 day, and (e, j) for +2 day.

TP down through eastern Asia and western Pacific into the central Pacific basin. It is noticeable that this wave train comes from southwest side of the TP in the STEA southern branch region at lag = −2 and −1 (Figs. 8a, b). At lag = +1 and +2 (Figs. 8d, e), the wave train moves away from the landmass and migrates further eastward. When it reaches the east of the dateline, the wave train becomes weak. Regarding the composite differences (Figs. 8f–j), the anomalous wave train appears over East Asia and its coastal regions during lag = −2 to lag = 0 period. However, it cannot propagate eastward further into the midlatitude North Pacific in the following two days.

Figure 9 displays the regression maps for the case of base point 2. Climatologically, the STEAs over the landmass migrate southeastward firstly along the STEA northern axis, and then move eastward into the oceanic region. The propagation distance connected with base point 2 is further east than that with base point 1 (see the central locations of the wave train in Fig. 9). The anomalous wave train moves eastward almost along its climatological track. Only the spatial phase shifts to higher latitudes and reaches the northwest coastal region of North America, after the anomalous wave train moves into the oceanic region. Therefore, the STEA anomalies over the oceanic region shown in Fig. 7b are partly attributed to the eastward propagation of the STEA anomalies over land. A similar process of lag-regression described above is used to explore the source of the STEA anomalies over the North Pacific region in Fig. 7. The results show that the climatological and anomalous wave trains bear close resemblance with those in Fig. 9. Therefore, the STEA anomalies accompanied by the East Asian jet stream anomalies can propagate as a wave train along the axis of the STEA northern branch into the East Asian coastal region, and extend further eastward into midlatitude North Pacific. However, the STEA anomalies, which are located near the axis of the STEA southern branch but far away from the northern branch, can only exist over the eastern part of East Asia and its coastal region at 200 hPa. Hence, the upstream "anomalous seeds" that affect the STEA over the North Pacific region (Orlanski, 2005) show a feature of regional selectivity.

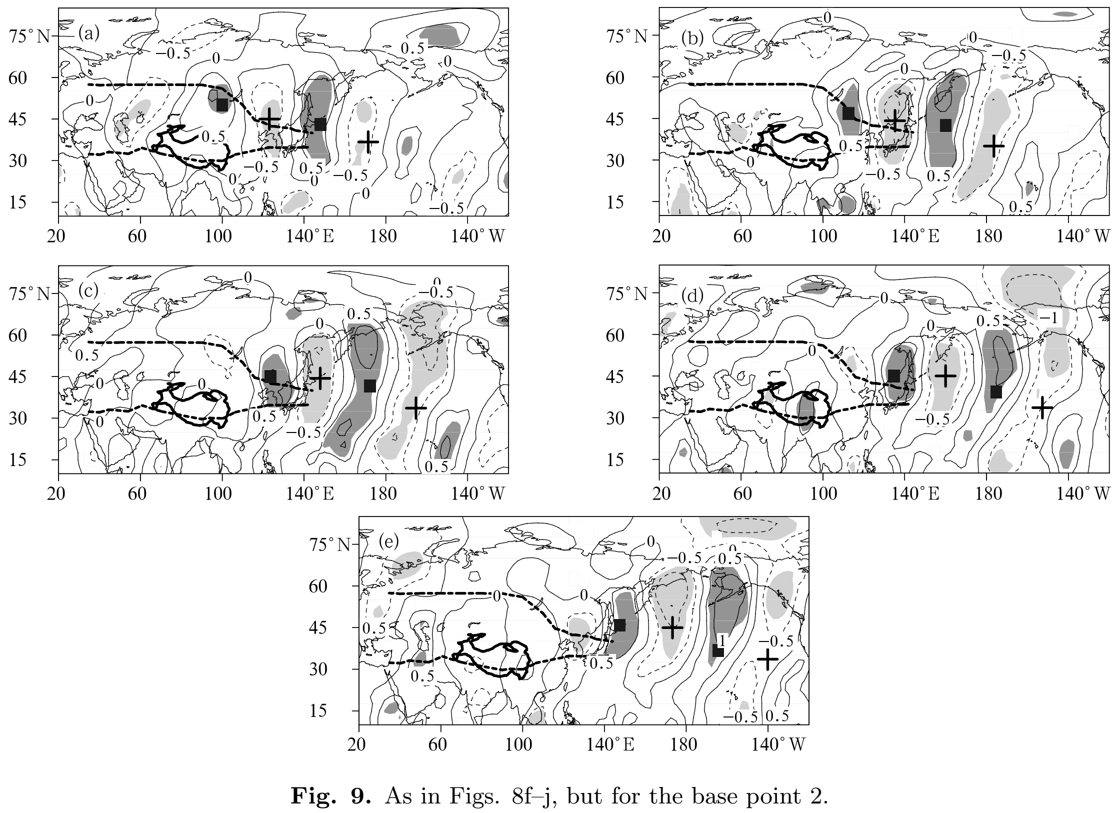

Fig. 9. As in Figs. 8f–j, but for the base point 2.

5. Conclusions and discussion

The ERA-40 reanalysis data are used to investigate the climatological features of the EASJ and EAPJ, as well as STEA in winter. The anomalous patterns of the EAPJ, the associated large-scale circulation, the STEA, and the STEA propagation features are also examined in this paper. The main conclusions are drawn as follows:

(1) The EASJ and EAPJ on the monthly mean field have no clear geographical border at the upper level. In addition, the EAPJ has no closed jet center in the monthly mean field. The distribution of the numbers of jet cores extracted from the daily data exhibits a distinct boundary in the latitudes of the northern part of the TP. There exist two lobes with large numbers of jet cores, corresponding to the EASJ and EAPJ regions. The spatial match of STEA with EASJ and EAPJ is as follows: the strong EASJ is located within the weak southern branch of the STEA, while the relatively weak EAPJ appears within the active northern branch of the STEA. The STEAs between the two branches are much suppressed.

(2) The winter EAPJ demonstrates two anomalous patterns. One is the anomalous anticyclonic/cyclonic circulation pattern in the EAPJ region. Simultaneously, the associated large-scale circulation anomalies are mainly concentrated in mid to high latitudes over the Eurasian region. Another is the weakening/strengthening of local westerly wind. The associated anomalous atmospheric circulation shows the Eurasian (EU) teleconnection pattern. The atmospheric circulation anomalies in the mid to high latitudes and over the upstream of East Asia may cause the circulation anomalies in the EAPJ region via influencing the temperature contrast between the mid-high latitude Eurasia and the subtropical regions.

(3) The anomalies of the winter EAPJ are also highly correlated with the STEA anomalies over East Asia. The anomalies in the northern branch of the STEA migrate eastward as a wave train along its axis into the East Asian coastal waters, and further into the oceanic region. However, the ones near the southern branch are trapped over the eastern part of East Asia and its coastal waters at 200 hPa.

As discussed above, our conclusions about the variations of the East Asian jet stream are consistent with those from previous studies. However, the current investigation on the relationship between jets and transient eddy activities based on the daily data and the transient eddy dynamics help to understand the features of the two jets over East Asia. The results demonstrate that the EAPJ is the jet that coexists with the STEA, which is distinct from the EASJ. Additionally, after the STEA anomalies propagate eastward into the oceanic region, they can influence the North Pacific climate anomalies through the thermal and dynamical feedbacks between the transient eddy and large-scale circulation. Thus, the connection between the climate anomalies over East Asia and those over the Pacific region are established through these processes.

REFERENCES

Carillo, A., P. M. Ruti, and A. Navarra, 2000: Storm tracks and zonal mean flow variability: A comparison between observed and simulated data. *Climate Dyn.*, **16**, 219–228.

Chang, E. K. M., 1993: Downstream development of baroclinic waves as inferred from regression analysis. *J. Atmos. Sci.*, **50**, 2038–2053.

Chen Haishan and Sun Zhaobo, 2003: The effects of Eurasian snow cover anomaly on winter atmospheric general circulation. Part I: Observational studies. *Chinese J. Atmos. Sci.*, **27**(3), 304–316. (in Chinese)

—, —, and Zhu Weijun, 2003: The effects of Eurasian snow cover anomaly on winter atmospheric general circulation. Part II: Model simulation. *Chinese J. Atmos. Sci.*, **27**(5), 847–860. (in Chinese)

Cressman, G. P., 1981: Circulations of the West Pacific jet stream. *Mon. Wea. Rev.*, **109**, 2450–2463.

Dong Min, Yu Jianrui, and Gao Shouting, 1999: A study on the variations of the westerly jet over East Asia and its relation with the tropical convective heating. *Chinese J. Atmos. Sci.*, **23**(1), 62–70. (in Chinese)

Gallego, D., P. Ribera, R. Garcia-Herrera, E. Hernandez, and L. Gimeno, 2005: A new look for the Southern Hemisphere jet stream. *Climate Dyn.*, **6**, 607–621.

Gao Shouting, Tan Shiyan, and Ding Yihui, 1989: Generalized E-P flux representing wave-mean flow interactions. *Sci. China (Ser. B)*, **7**, 774–784. (in Chinese)

Hou, A. Y., 1998: Hadley circulation as a modulator of the extratropical climate. *J. Atmos. Sci.*, **55**, 2437–2457.

Jhun, J. -G., and E. -J. Lee, 2004: A new East Asian winter monsoon index and associated characteristics of the winter monsoon. *J. Climate*, **17**, 711–726.

Kuang Xue-Yuan and Zhang Yao-Cun, 2006: Impact of the position abnormalities of the East Asian subtropical westerly jet on summer precipitation in the middle-lower researches of the Yangtze River. *Plateau Meteor.*, **25**(3), 382–389. (in Chinese)

Li Chongyin, Wang Jough-Tai, Lin Shi-Zhei, and Cho Hun-Ru, 2004: The relationship between East Asian summer monsoon activity and northward jump of the upper westerly jet location. *Chinese J. Atmos. Sci.*, **28**(5), 641–658. (in Chinese)

Li Jian, Rucong Yu, Tianjun Zhou, et al., 2005: Why is there an early spring cooling shift downstream of the Tibetan Plateau? *J. Climate*, **18**(22), 4660–4668.

Liao Qinghai, Gao Shouting, Wang Huijun, and Tao Shiyan, 2004: Anomalies of the extratropical westerly jet in the Northern Hemisphere and their impacts on East Asian summer monsoon climate anomalies. *Chinese J. Geophys.*, **47**(1), 10–18. (in Chinese)

Lim, G. H., and J. M. Wallace, 1991: Structure and evolution of baroclinic waves as inferred from regression analysis. *J. Atmos. Sci.*, **48**, 1718–1732.

Mao Rui, Gong Daoyi, and Fang Qiaomin, 2007: Influence of the East Asian jet stream on winter climate in China. *J. Appl. Meteor. Sci.*, **18**(2), 137–146. (in Chinese)

Orlanski, I., 2005: A new look at the Pacific storm track variability: Sensitivity to tropical SSTs and to upstream seeding. *J. Atmos. Sci.*, **62**, 1367–1390.

Ren Xuejuan and Zhang Yaocun, 2007: Western Pacific jet stream anomalies at 200 hPa in winter associated with oceanic surface heating and transient eddy activity. *Acta Meteor. Sinica*, **21**(3), 277–289.

Sheng Chengyu, 1986: *An Introduction to the Climate of China*. Science Press, Beijing, 85–89 pp.

Sun Li, An Gang, Liang Yi, et al., 2002: The unusual characteristics of general circulation in drought and water logging years of Northeast China. *Climatic and Environmental Research*, **7**(1), 102–113. (in Chinese)

Tao Zuyu and Hu Aixue, 1994: Climatological analysis of transient eddy in the northern winter. *Chinese J. Atmos. Sci.*, **18**(3), 320–330. (in Chinese)

Teresa, M. B., E. H. Atallah, L. F. Bosart, et al., 2001: The wintertime Southern Hemisphere split jet: Structure, variability, and evolution. *J. Climate*, **14**, 4191–4215.

Thompson, D. W., and J. M. Wallace, 1998: The Arctic oscillation signature in the winter geopotential height and temperature fields. *Geophys. Res. Lett.*, **25**(9), 1297–1300.

Uppala, S. M., P. W. Kållberg, A. J. Simmons, et al., 2005: The ERA-40 reanalysis. *Quart. J. Roy. Meteor. Soc.*, **131**, 2961–3012.

Wallace, J. M. and D. S. Gutzler, 1981: Teleconnection in the geopotential height field during the Northern Hemisphere winter. *Mon. Wea. Rev.*, **109**(4), 784–812.

Wang Xiaoman, Ding Zhiying, and Zhang Xingqiang, 2002: Statistic and dynamic analysis to the relation between Meiyu storm and high level jet. *J. Nanjing Inst. Meteor.*, **25**(1), 111–117. (in Chinese)

Watanabe, M., 2004: Asian jet waveguide and a downstream extension of the North Atlantic oscillation. *J. Climate*, **17**, 4674–4691.

Wu Weijie, He Jinhai, Hyo-Sang Chung, et al., 2006: The relationship between the East Asian upper-tropospheric jet stream in summer and climatic characteristics of synoptic-scale disturbances. *Climatic and Environmental Research*, **11**(4), 525–534. (in Chinese)

Xin Xiaoge, Rucong Yu, Tianjun Zhou, and Bin Wang, 2006: Drought in late spring of South China in recent decades. *J. Climate*, **19**(13), 3197–3206.

Yang, S., K. M. Lau, and K. M. Kim, 2002: Variation of the East Asian jet stream and Asian-Pacific-American winter climate anomalies. *J. Climate*, **15**, 306–325.

Ye Duzheng, Tao Shiyan, and Li Maicun, 1958: The abrupt change of circulation over Northern Hemisphere during June and October. *Acta Meteor. Sinica*, **29**(4), 250–263. (in Chinese)

Yu Rucong and Zhou Tianjun, 2004: Impacts of winter-NAO on March cooling trends over subtropical Eurasia continent in the recent half century. *Geophys. Res. Lett.*, **31**, L12204, doi: 10.1029/2004GL019814.

—— and ——, 2007: Seasonality and three dimensional structure of the interdecadal change in East Asian monsoon. *J. Climate*, **20**(21), 5344–5355.

Zhang, Y., X. Kuang, W. Guo, and T. Zhou, 2006: Seasonal evolution of the upper-tropospheric westerly jet core over East Asia. *Geophys. Res. Lett.*, **33**, L11708, doi: 10.1029/2006GL026377.

Zhou Bing, Han Gui-rong, and He Jin-hai, 2003: Numerical experiment of effects of the upper level westerly jet on a torrential rain over the middle-lower reaches of the Yangtze River. *J. Nanjing Inst. Meteor.*, **26**(5), 595–604.

Zhu Weijun and Sun Zhaobo, 2000: Interannual variability of northern winter Pacific storm track and its association with 500 hPa height and tropical and northern Pacific sea surface temperature. *Acta Meteor. Sinica*, **58**(3), 309–320. (in Chinese)

Zou Jinshang, Jiang Jing, and Wang Meihua, 1990: *Climatology in the Upper Atmosphere.* China Meteorological Press, Beijing, 200–212pp.